

Article

Safety Control Technology and Monitoring Analysis for Shield-Tunnel-Stacked Underpass High-Speed Rail Bridge Excavation

Taihua Yang ¹, Xiaoxiang Peng ¹, Xing Huang ², Bin Liu ^{2,*}, Kejin Li ³, Jianyong Zhang ^{3,4}, Yixiang Li ^{3,4} and Tian Wen ¹

¹ School of Urban Construction, Wuhan University of Science and Technology, Wuhan 430065, China; yangtaihua@wust.edu.cn (T.Y.); 13618482731@163.com (X.P.)

² State Key Laboratory of Geomechanics and Geotechnical Engineering, Institute of Rock and Soil Mechanics, Chinese Academy of Sciences, Wuhan 430071, China; xhuang@whrsm.ac.cn

³ China Railway 14th Bureau Group Co., Ltd., Jinan 250101, China

⁴ China Railway 14th Bureau Group Shield Engineering Co., Ltd., Nanjing 210000, China

* Correspondence: liubin@whrsm.ac.cn

Abstract: In order to ensure the safety of the Beijing–Shanghai high-speed railway during the construction and operation of the shield tunnel on Line R1 of the Jinan Metro, a numerical simulation of geological disturbance during the underpass of the small-radius stacked tunnel was carried out. We analyzed the mechanism of geological deformation and the construction factors affecting settlement and found that bridge settlement far exceeded safety standards without taking safety control measures. In this regard, safety control technologies such as setting isolation pile sleeve valve pipes, controlling shield tunneling parameters, grouting control technology, and trolley support technology have been proposed. Monitoring was conducted on the uneven settlement of the bridge surface, the internal and external stresses of the pipe segments, and the soil pressure they were subjected to. The results showed that the surface settlement of the bridge after safety control measures was controlled within the safety standard range, and the stress and soil pressure changes of the pipe reinforcement were within the allowable range, further verifying the effectiveness of the safety control measures.

Keywords: stacked tunnel; shield tunneling; numerical simulation; security control; on-site monitoring



Citation: Yang, T.; Peng, X.; Huang, X.; Liu, B.; Li, K.; Zhang, J.; Li, Y.; Wen, T. Safety Control Technology and Monitoring Analysis for Shield-Tunnel-Stacked Underpass High-Speed Rail Bridge Excavation. *Appl. Sci.* **2024**, *14*, 1699. <https://doi.org/10.3390/app14051699>

Academic Editors: Asterios Bakolas and Roberto Camussi

Received: 18 December 2023

Revised: 23 January 2024

Accepted: 8 February 2024

Published: 20 February 2024



Copyright: © 2024 by the authors. Licensee MDPI, Basel, Switzerland. This article is an open access article distributed under the terms and conditions of the Creative Commons Attribution (CC BY) license (<https://creativecommons.org/licenses/by/4.0/>).

1. Introduction

The construction of underground projects such as subways has become the best strategy to alleviate traffic pressure. Due to the lack of long-term, forward-looking urban planning, the new subway tunnel will inevitably be unavoidable in crossing the existing architectural structure.

To this end, domestic and foreign scholars have carried out a lot of research on the formation deformation induced by shield construction and achieved rich research results. Some scholars have carried out a lot of valuable work on the research of near construction, surface settlement, and tunnel longitudinal deformation [1–5]. The research methods for inducing geological deformation during shield tunneling mainly include the empirical formula method, the analytical method, numerical simulation, and on-site measurement. On the basis of obtaining the field observation data, Peck [6] used mathematical statistical methods and considered certain construction conditions to derive an empirical formula for geological deformation. After Peck, scholars combined engineering practice and continuously improved their previous research work, achieving a large number of research results. Chen [7] fully considered the impact of new tunnel construction on existing tunnels and the different arrangements of excavation surfaces for double-track tunnels and constructed a modified three-dimensional Peck formula. Cirong et al. [8] studied the resistance

to deformation of large-diameter tunnels, analyzed the influencing factors of settlement sources, and proposed control techniques such as post-construction grouting repair and temporary steel support. Wang [9] obtained the Peck formula based on the superposition principle, relying on the engineering background of Nanning Metro Line 1, Line 2, and Line 4 parallel underpass train station tracks. Osman [10,11] proposed a modified Gaussian curve to predict displacement on the surface and in the ground and represented the ground subsidence caused by the interaction between double tunnel tunnels using the modified Gaussian curve. The analytical method mainly considers the soil as a continuous medium and uses mathematical mechanics to describe the impact of shield tunneling on geological deformation. It mainly includes elasticity theory, elastic-plastic theory, viscoelasticity theory, and so on. Based on the one-dimensional consolidation theory of Terzaghi, Wei [12] fully considered the consolidation settlement mechanism and drainage conditions of the soil around the tunnel and obtained the calculation formula for soil consolidation settlement after tunnel construction is completed. Using a Boussinesq solution based on elastic half space, Wei [13] established a simplified model of conical disturbance load acting on a circular plane, derived a simplified formula for the maximum ground settlement caused by the shield tunnel construction stage, and analyzed the influence of two important parameters in the formula on the maximum settlement value. Numerical simulation is an application of mathematics. Numerical simulation is essentially applied mathematics, and with the development of information and computing technology, numerical simulation technology continues to mature. Based on K. M., the equivalent formation loss parameter method proposed by Lee et al., Wang [14] used numerical simulation methods to study the intrinsic relationship between settlement changes during shield tunnel construction and two important shield parameters (face pressure and grouting pressure) and proposed a calculation method for the influence of shield parameters on tunnel settlement. Teng [15] relied on the Chengdu Metro tunnel project and used the PFC2D two-dimensional particle flow program and Plaxis 3D finite element software to numerically simulate shield tunneling through sandy and gravel layers, revealing the instability mechanism and surface settlement characteristics of the excavation surface of shield tunneling through sandy and gravel layers. Takahashi [16] proposed adopting a refined construction control plan, including reinforcement grouting of the strata during excavation and strengthening monitoring of building deformation during construction. Takahashi [16] proposed adopting a refined construction control plan, including reinforcement grouting of the strata during excavation, strengthening monitoring of building deformation during construction, and ultimately controlling the settlement of the building within 4 mm. Sirivachiraporn [17] monitored the entire construction process of Bangkok Metro Line 1 in Thailand and found that the surface settlement in most sections was within 20–40 mm, equivalent to 0.5–2.0% of the lost volume of the formation. Francesco Basile [18] proposed an analysis method for calculating the impact of tunnel excavation on existing pile foundations. Pornkasem Jongpradist [19] studied the effect of tunnel excavation on existing load-bearing pile foundations by establishing a three-dimensional elastic-plastic numerical simulation model. Loganathan [20] conducted centrifugal model tests to simulate the lateral penetration of pile foundations during shield tunneling construction. F. Leung [21] and D. E. L. Ong [22] conducted centrifugal model tests, setting up six reference groups, including two, four, and six pile foundations composed of cap and non-cap pile foundations, to study the effect of the number of caps and pile groups on the deformation of the pile body during excavation. However, currently there are relatively few research cases on high-speed railway bridges with high sensitivity to lateral deformation during shield tunneling of small-radius stacked tunnels. In most studies, simulation studies were not conducted in advance based on the actual engineering situation of the project, which did not fully reflect the actual engineering characteristics. There is insufficient understanding of safety protection measures for buildings with high sensitivity when passing through small-radius stacked tunnels.

Therefore, this article takes the shield tunneling under the pile foundation of the Beijing–Shanghai high-speed railway bridge group between Wangfuzhuang Station and

Dayangzhuang Station on Jinan Metro Line R1 as the engineering background. We established a shield tunneling model based on on-site survey data and simulated the disturbance of shield tunneling under normal excavation conditions. Furthermore, we analyzed the deformation mechanism and influencing factors of the strata and took targeted safety control and reinforcement measures before shield tunneling construction based on simulation results. We set up monitoring points on the surface and bridge piers along the line. Moreover, we verified the effectiveness of safety reinforcement measures through on-site monitoring results and provided case reference and technical support for the on-site construction of small-radius stacked tunnels crossing highly sensitive buildings.

2. Project Overview

Jinan Metro Line R1 runs 624 m east of Wangfuzhuang Station. The shield tunneling machine passes under the Beijing–Shanghai high-speed railway at the down line mileage K412 + 119.77~K412 + 183.77 (corresponding to the up line mileage K6 + 018~K6 + 082 of the Beijing–Jinan connecting line and the down line mileage K7 + 106~K7 + 170 of the Beijing–Jinan connecting cable). The left and right lines of the shield tunnel section are diagonally crossing the elevated bridge piles of the Beijing–Shanghai high-speed railway between Piers 104 and 105, as shown in Figure 1. The left and right tunnels adopt a stacking method, with a stacking length of 210 m. The minimum clear distance between the left and right lines is 3.2 m, and the curve radius of the underpass section of the tunnel is about 300 m, as shown in Figure 2.

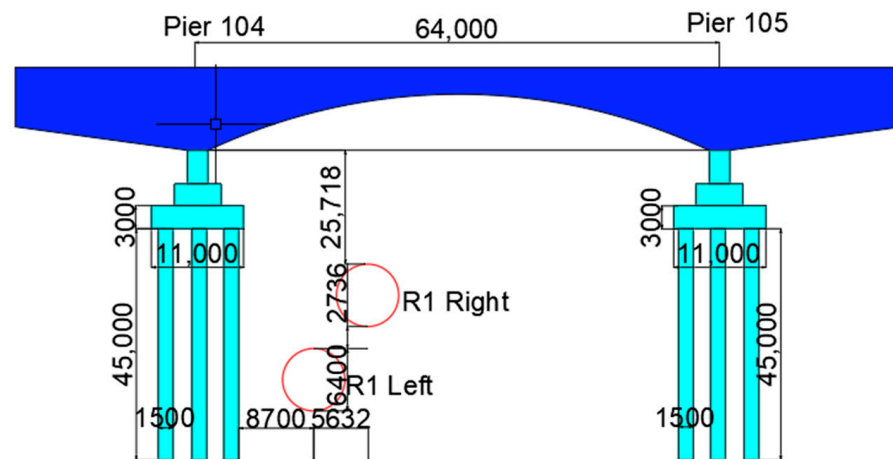


Figure 1. Cross-section of R1 underpasses the Beijing–Shanghai high-speed railway section.

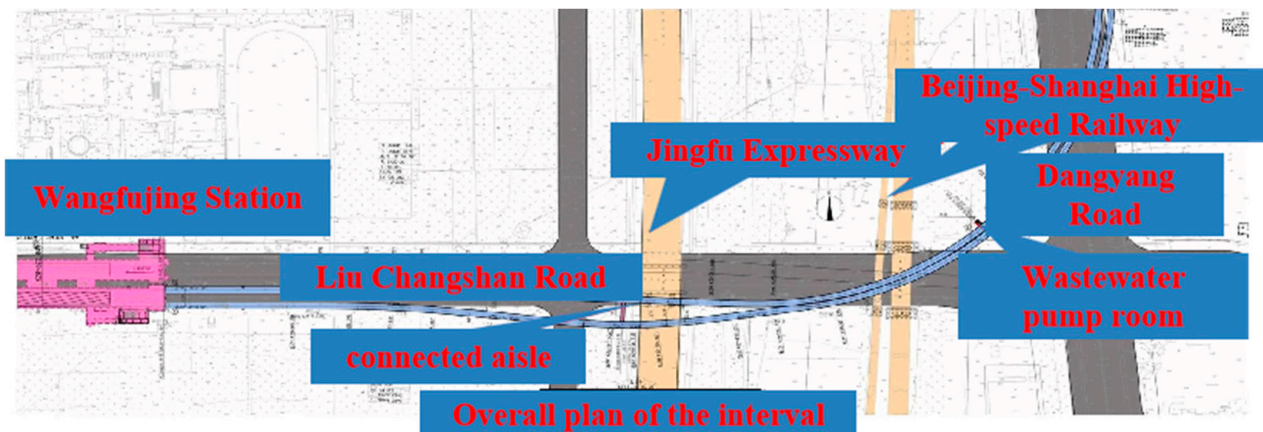


Figure 2. General plan of small-radius turning interval.

The soil cover thickness of the shield tunneling section on the left and right lines is 28.35 m and 19.22 m, respectively, with an outer diameter of 6.4 m, an inner diameter of 5.8 m, and a lining thickness of 0.3 m. The left tunnel of the underpass section is mainly located in the silty clay and pebble layers. In contrast, the proper tunnel is primarily located in the silty clay and delicate sand layers. The specific geotechnical parameters are shown in Table 1. The difficulty lies in the complex working conditions (considerable burial depth, high soil and water pressure, sand and gravel, slight radius curve turning, and stacking), an underpass of the Beijing–Shanghai high-speed railway, rigorous dynamic load, and deformation requirements (settlement < 1 mm).

Table 1. Statistics of rock and soil mechanics parameters in the Jinan shield tunnel construction section.

Rock Soil Stratification	Soil Thickness (m)	Modulus of Elasticity (MPa)	Poisson Ratio	Severe (kN/m ³)	Internal Friction Angle (°)	Cohesive Strength (kPa)
Miscellaneous fill ①1	5.9	4.3	0.35	18.5	18.3	20
Fine sand ⑦	4.1	18	0.29	20.8	20	0
Loess ⑦	9.8	5.6	0.26	19.1	23	43
Silty clay ⑧	12.7	6.5	0.23	19.4	22	47
Silty clay ⑩	10.3	7.8	0.25	19.2	24	50
Pebble ⑩1	8.5	40	0.23	21.0	35	0
Silty clay ⑪	13	8.1	0.28	19.4	24	52
Pebble ⑪1	15.7	45	0.23	21.2	40	0

3. Mechanism of Disturbance and Deformation in the Stratum of Shield Tunnels Undercrossing High-Speed Rail Bridges

3.1. Model Establishment

Numerical simulation was conducted using ABAQUS2023 finite element software, taking into account factors such as grouting pressure, equivalent layer thickness, tunnel spacing, and soil chamber pressure. To eliminate the influence of boundary effects, the calculation model has a length of 150 m in the x direction, 100 m in the y direction, and 80 m in the z direction. The lower surface and surrounding boundaries of the soil model adopt vertical constraints, while the upper surface adopts free boundaries. The surface of the bridge pier has free boundaries. Considering that the pile foundation of the high-speed railway bridge is an end-bearing pile with no contact surface between the pile side and the surrounding soil, the bottom of the pile end and the bearing layer soil adopt a tangential rough normal “hard” contact model. A small-radius stacked tunnel underpass high-speed rail model was constructed to simulate the shield tunneling construction process, as shown in Figure 3. The basic model material parameters are shown in Table 2.

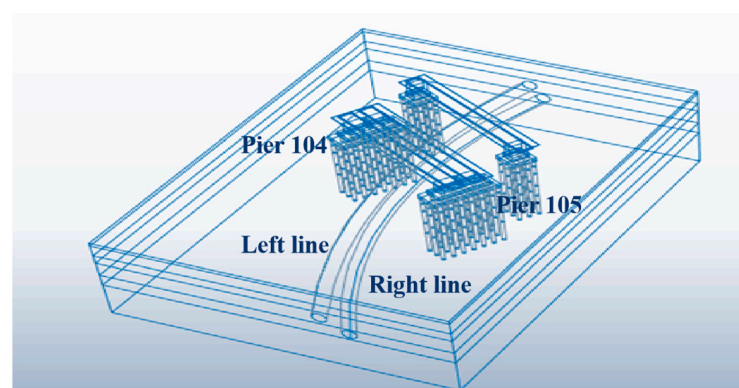


Figure 3. Small-radius stacked tunnel underpassing a high-speed rail model.

Table 2. Basic model of material parameters.

Title	Severe (kN/m ³)	Elastic Modulus (GPa)	Poisson's Ratio	Outside Diameter (m)	Inner Diameter (m)	Thickness (m)
Tunnel lining	30	40	0.3	6.4	6	0.2
Isogenerational layer	20	0.03	0.25	6.4	6.475	0.075
Shielding	80	210	0.3	6.4	6	0.2
Bridge piers and piles foundations	30	35	0.3	/	/	/

3.2. Disturbance Simulation under Normal Excavation Conditions

From the simulated cumulative settlement curve in Figure 4, it can be seen that construction parameters such as soil silo pressure and grouting pressure are fully considered. Construct a high-precision three-dimensional numerical simulation model for the pile foundation of the Beijing–Shanghai high-speed railway bridge group under the construction of a high-stacked tunnel. The specific settlement deformation is shown in Figure 5. The calculation results indicate that as the shield tunneling construction continues to advance, the cumulative settlement value of the bridge piers ultimately exceeds the warning value by 1 mm. If safety control measures are not taken during shield tunneling construction, it will seriously affect the bridge structure and geological deformation, posing great safety hazards to the safe operation of high-speed railway lines.

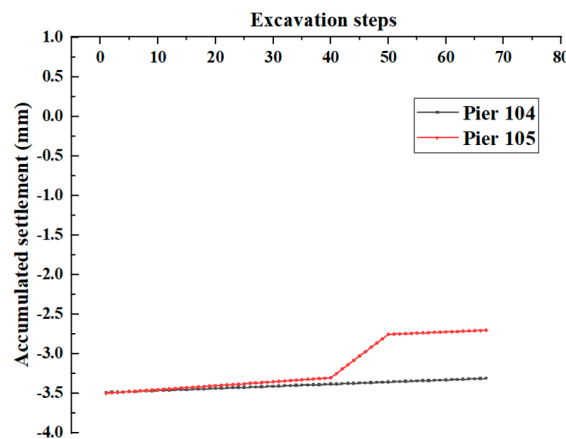


Figure 4. Accumulated settlement curve of the elevated bridge under normal excavation conditions.

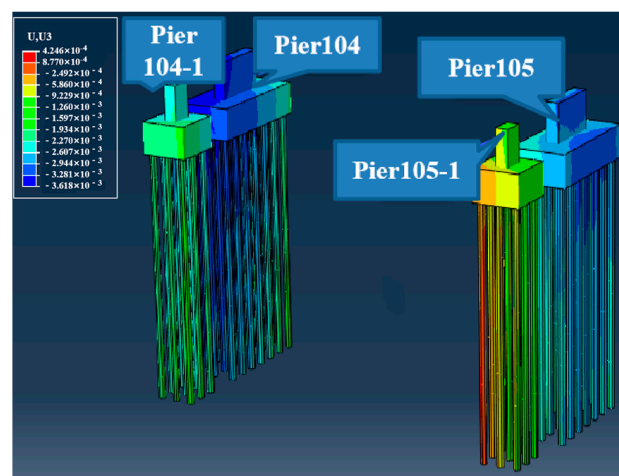


Figure 5. Settlement deformation diagram of an elevated bridge under normal excavation conditions.

3.3. Mechanism of Pile–Soil Interaction during Shield Tunneling under Bridge Construction

During the process of tunneling through existing bridge pile foundations, the tunnel, strata, and bridge pile foundations are interdependent and mutually influential. Figure 6 reveals the relationship between the three. Subway shield tunneling is the source of construction disturbance; the stratum is the medium for transmitting construction disturbance; and the bridge pile foundation is the carrier for bearing construction disturbance. The tunnel, strata, and bridge pile foundations ultimately form a dynamic equilibrium. Shield tunneling construction is accompanied by the release of soil stress, resulting in stress redistribution within a certain range of the strata and causing certain disturbances to the surrounding strata, which directly manifest as deformation of the strata at a macro level. When the deformation of the local layer is transmitted to the vicinity of the bridge pile foundation, the changes in the mechanical parameters of the soil and the internal stress state of the stratum have a profound impact on the bearing capacity of the bridge group pile foundation. Even negative frictional resistance is generated on the pile side, causing uneven settlement of the bridge structure, resulting in structural tilting, cracks, and other phenomena. Meanwhile, the presence of bridge pile foundations further hinders the further transmission of geological deformation.

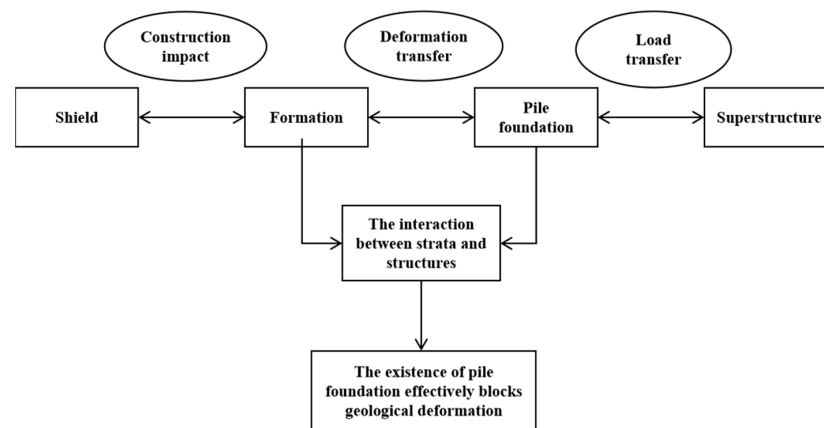


Figure 6. Mechanism of interaction between shield tunneling, piles, and soil.

3.4. Construction Factors Affecting Building Settlement

3.4.1. Soil Warehouse Pressure

During shield tunneling, maintaining a balance between the soil pressure in the soil chamber and the water and soil pressure on the working face is a significant factor in preventing surface subsidence and ensuring building safety. The adjustment of soil storage pressure should be based on feedback from geological conditions, burial depth, and surface settlement during tunnel excavation. By adjusting the tunnel excavation speed, screw conveyor speed, and other methods, a balance can be achieved between the amount of excavation in each loop and the amount of soil discharged.

3.4.2. Shield Tunneling Parameters

The excavation parameters for shield tunneling construction include excavation mode, jack thrust, excavation speed, cutterhead torque, and cutterhead speed. The changes in these parameters have a significant impact on shield tunneling construction and ground settlement. In weak areas and areas with poor geological conditions, the mode of soil pressure balance should be adopted as much as possible. Ensure that the pressure in the soil silo is balanced with the combined force of soil and water on the palm surface. The jack thrust, propulsion speed, cutterhead torque, and cutterhead speed should be controlled within a reasonable parameter range. Excessive excavation parameters will increase disturbance to the formation and settlement. If the excavation parameters are too small, it will increase the time for the shield machine to pass under the building, thereby

increasing the spatiotemporal effect of shield excavation on the formation. Therefore, controlling the excavation parameters well is the key to controlling geological subsidence and its impact on buildings.

3.5. Safety Control Standards for High-Speed Railway Bridges

We discussed the standards and regulations for the operation and management of high-speed railway lines and analyzed actual engineering cases of shield tunneling adjacent to the construction of underpass bridges. Combined with the actual engineering overview of the Jinan R1 Line under the Beijing–Shanghai high-speed railway bridge. According to the “Special Design of Jinan Rail Transit R1 Line Project Undercrossing the Beijing Shanghai High Speed Railway”, risk control is divided into three levels of early warning. The settlement standard for bridge piers is controlled at 1 mm, and the surface deformation standard is controlled at 20 mm. Yellow, orange, and red warning levels are set at 50%, 75%, and 90% of the allowable settlement value, respectively. This article proposes safety control standards for the construction of stacked tunnel shield tunneling under existing high-speed railway bridges, as shown in Table 3.

Table 3. Safety control standards for shield tunneling construction of the Jinan Metro R1 Line undercrossing existing high-speed railway bridges.

Monitoring Projects	Yellow Alert		Orange Alert		Red Alert		Limit	
	Change Rate (mm/Day)	Accumulated Settlement (mm)	Change Rate (mm/Day)	Accumulated Settlement (mm)	Change Rate (mm/Day)	Accumulated Settlement (mm)	Change Rate (mm/Day)	Accumulated Settlement (mm)
Bridge pier settlement	±0.36	±0.5	±0.45	±0.75	±0.54	±0.9	±0.9	±1.0
Surface subsidence	±5	±10	±8	±15	±10	±18	±15	±20.0

3.6. Construction Safety Control Technology

It has been obtained from the simulation results of normal excavation conditions that the shield tunneling under the elevated bridge will cause settlement interference on the bridge body that far exceeds the warning line. There are significant safety hazards in the normal operation of railway lines. Therefore, necessary safety control measures must be taken during shield tunneling construction to reduce disturbance to the surrounding soil.

3.6.1. Setting up Isolation Piles and Sleeve Valve Pipes

1. To ensure the safety of the Beijing–Shanghai high-speed railway during the construction and operation of shield tunnels, a pile foundation is installed between the bridge foundation of the Beijing–Shanghai high-speed railway and the shield tunnel (Φ 800@1000). Isolation and protection of drilled cast-in-place piles. The minimum distance between the isolation pile and the pile foundation of the existing Beijing–Shanghai high-speed railway bridge is 8.7 m, as shown in Figure 7. Considering the operational safety of the Beijing–Shanghai high-speed railway and the actual construction clearance on site, the drilling and grouting piles are selected to be drilled using a positive circulation drilling rig. The positive circulation drilling rig is 6 m high, with the most unfavorable position located under the bridge on the north side of the high-speed railway as an example. The drilling rig is 3.4 m away from the bottom of the beam, which does not pose a safety hazard to the crane. The pile foundation is drilled using manual lifting of steel cages, which are made in eight sections with a single section length of 5 m. The concrete pouring is carried out using the conduit method, which does not pose any safety hazards to the driver.
2. Sleeve valve pipe construction. Sleeve valve pipes are used for grouting reinforcement in areas where drilling and grouting piles cannot be constructed due to pipelines. A

rigid sleeve valve pipe with a diameter of 40 mm and a backward segmented grouting method were adopted. The grouting spacing between sleeve valve pipes is 1.2 m, and the grouting material within the reinforcement range is cement and water glass double liquid slurry. The sleeve valve pipe is drilled using a drilling rig, with two on the south side and a height of 5 m. The construction location is on the outside of the bridge and the west side of the high-voltage line, which does not pose a safety hazard to the driver.

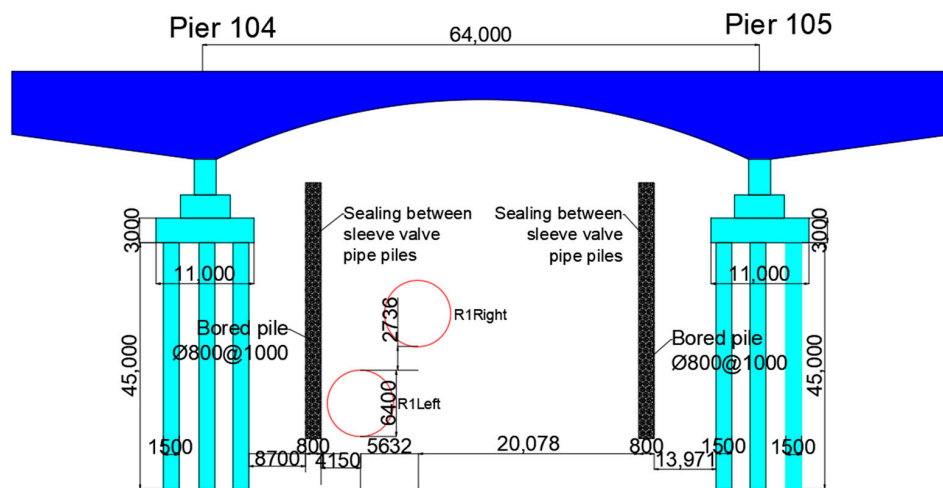


Figure 7. Isolation piles and sleeve valve pipes.

To reduce the difficulty of shield tunneling construction and consider the impact of shield tunneling on bridge pile foundations. Reserve grouting pipes on both sides of the isolation pile to achieve water sealing between the piles. The isolation piles on the outer side of the bridge that cannot be implemented due to pipeline relocation have been adjusted to sleeve valve pipe grouting to block the transmission of groundwater in the middle, fine sand layer, and pebble layer.

3.6.2. Optimization and Control of Shield Tunneling Parameters

The setting of excavation parameters during shield tunneling construction is a prerequisite for ensuring the progress of shield tunneling construction and ground settlement control. To minimize the impact of shield tunneling passing through the elevated bridge, it is recommended to pass through the disturbance range of the bridge continuously and quickly. Before the shield tunneling passes through the Beijing–Shanghai high-speed railway, the section below the Beijing–Taiwan expressway was selected as the shield tunneling simulation test section. At the same time, based on the measured data of the experimental section, we optimized various propulsion parameters and strictly controlled the propulsion speed of the shield machine. We ensured synchronous grouting volume and secondary grouting and tried to reduce the ground settlement caused by shield tunneling. To ensure the accuracy of excavation parameters, combined with domestic and foreign shield tunneling construction experience and our own construction examples, the excavation parameters of shield tunneling were calculated and selected. The specific details are shown in Table 4.

Table 4. Adjustment of shield tunneling parameters.

Parameter	Trial excavation standards
Soil pressure	Upper soil pressure 1.5~2.0 bar
Total thrust	800~2000 T
Knife disc torque	1000~2500 KN·m
Advance speed	30~50 mm/min

Table 4. *Cont.*

Knife disc speed	0.8–1.0 rpm
Synchronous grouting pressure	0.1–0.3 MPa
Synchronous grouting volume	5.2 m ³
Excavated quantity	Not more than 56 m ³

3.6.3. Grouting Control Technology

(1) Synchronous grouting

The excavation sequence of shield tunneling is from the left line to the right line, and synchronous grouting is carried out during excavation. Cement mortar is selected as the synchronous grouting slurry, mainly composed of cement, hydrated lime, fly ash, bentonite, sand, and water. The setting time is controlled within 4–8 h, with high strength in the early and late stages. According to the geological conditions and excavation speed, the setting time is adjusted by adding accelerators and changing the ratio through on-site testing. For areas with strong permeability and high early strength requirements for grouting, the ratio and early strength agent added are further adjusted through on-site testing to shorten the setting time and ensure a good grouting effect. The grouting pressure is set at 0.3 MPa, and the filling coefficient is set at 1.3–2.5, which can be adjusted according to the actual situation on the construction site. According to shield tunneling construction experience, the grouting amount is taken as 130% to 250% of the gap in the shield tail building. The synchronous grouting speed should match the excavation speed, and the average grouting speed should be determined based on the amount of grouting completed within the 1.2-m excavation time of the shield machine in order to achieve uniform grouting.

(2) Secondary grouting

Secondary grouting is an effective auxiliary method to reduce surface subsidence. After completing the assembly of about 10 rings in the shield tunnel, inject secondary (or multiple) grouting into the lining ring, as shown in Figure 8, to compensate for the shortcomings of synchronous grouting. On the basis of synchronous grouting, cement water glass dual liquid slurry needs to be injected to control ground settlement. For this purpose, cement water glass dual liquid grouting was carried out through ground drilling holes with a secondary grouting slurry ratio of water/water glass = 3:1 (weight ratio); cement slurry/water cement ratio = 1:1 (weight ratio); and cement slurry/water glass slurry ratio = 1:1 (volume ratio). The grouting pressure is 0.3–0.4 MPa, and secondary grouting is carried out after 5–10 rings of shield tail detachment. The grouting amount is dynamically adjusted based on on-site settlement monitoring data.



Figure 8. Grouting hole.

3.6.4. Vehicle Support Technology

The excavation sequence of shield tunneling is first on the left line and then on the right line. During the construction of the left line and then on the right line, a trolley support system is set up inside the left line to protect the downstream tunnel. The trolley travels on the steel rail, with each track supported by five wheel supports, as shown in Figure 9. Under external thrust, the trolley can move forward longitudinally without unloading its force, reducing disturbance to the surrounding soil.

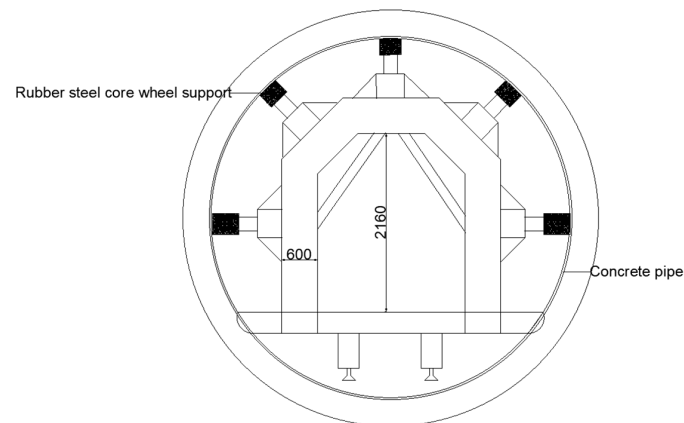


Figure 9. Schematic diagram of the support trolley.

4. Analysis of On-Site Monitoring Results of Shield Tunneling under High-Speed Railway Bridges

4.1. Monitoring Plan

Set up settlement observation points (Figure 10) and embed steel reinforcement gauges (Figure 11) and earth pressure gauges (Figure 12) inside the segments to monitor the surface settlement of the up and down line mileage K412 + 79.77~K412 + 223.77 of the Beijing–Shanghai high-speed railway, as well as the steel reinforcement stress and earth pressure on the 532 and 534 ring segments under the viaduct. Settlement monitoring is carried out by setting monitoring points and reference points to observe settlement points within the measuring station. The stress of steel bars and soil pressure in the pipe segments are automatically monitored and stored every 10 min using the DataTaker DT80G data acquisition instrument (Thermo Fisher Scientific, Waltham, MA, USA). Ground settlement, pipe stress, and changes in soil pressure on the pipe are important bases for the stability analysis of the structure of the R1 Line passing through the Beijing–Shanghai high-speed railway tunnel.

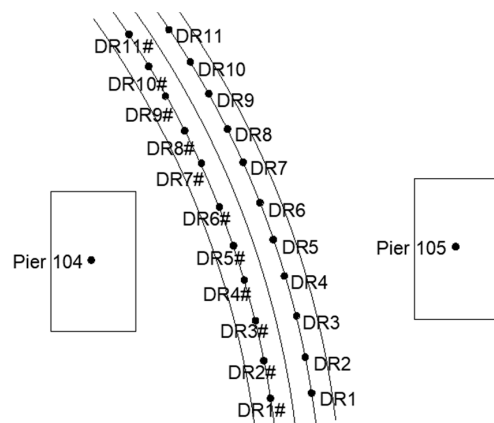


Figure 10. Distribution map of monitoring points in the section of the R1 line crossing the Beijing–Shanghai high-speed railway bridge.

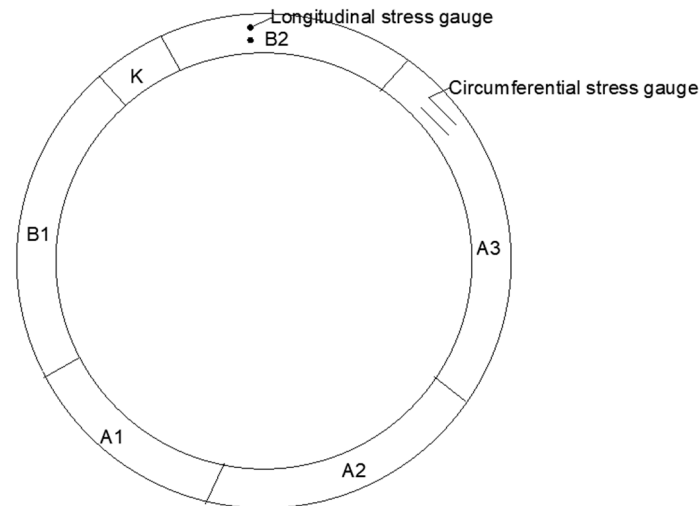


Figure 11. Schematic diagram of stress and soil pressure gauge measurement point layout.

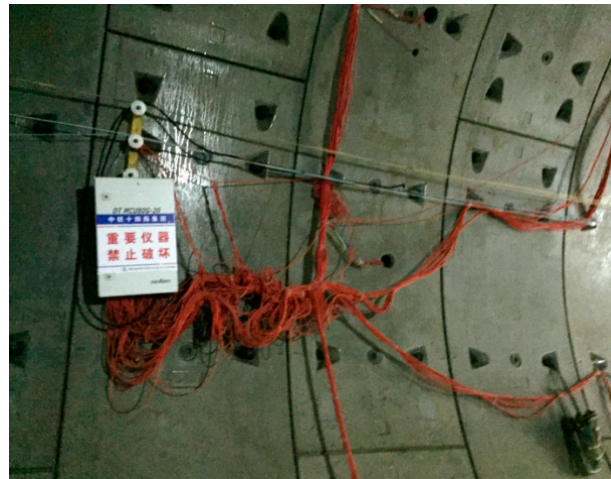


Figure 12. Automated real-time monitoring and early warning system.

4.2. Analysis of Monitoring Results

4.2.1. Analysis of Surface Subsidence Monitoring Results

Set up surface settlement monitoring points along the elevated bridge for shield tunneling and monitor the surface settlement of the left and right tunnel lines when the shield tunneling passes through the left and right pipes. The monitoring results are as follows:

The surface settlement along the process of the left and right shield tunneling passing through the elevated bridge is shown in Figures 13 and 14. During the process of shield tunneling crossing the left or right line, the settlement of Piers 104 and 105 always fluctuates within the range of (1, 1) mm. The maximum settlement did not exceed ± 1 mm, which meets the safety control standards. In the final settlement curve of the measuring points along the left line, the overall trend shows a slight uplift, followed by accelerated settlement, and finally a slow and stable decline. The upwelling part in the early stage mainly fluctuates within a range of 1 mm, and as the shield tunneling passes through, the surface settlement rapidly decreases to -4 mm. Subsequently, during the rapid descent phase, the disturbance of the shield tunnel to the soil gradually decreases. In the later monitoring period, the fluctuation gradually decreased from -4 mm to -6 mm and finally maintained a steady-state fluctuation. The overall change in surface subsidence was within the range of (1, -7) mm, which has not yet reached the yellow warning stage and meets safety control standards. The overall settlement process of the right line is similar to that

of the left line. The difference is that the downward trend of settlement on the right track is relatively slow, and the overall variation is more uniform due to the influence of shield tunneling. The final settlement value is also lower than the left line, only reaching about -5 mm. The overall variation of surface settlement is within the range of $(0, -7)$ mm. It has not yet reached the yellow warning stage and meets safety control standards.

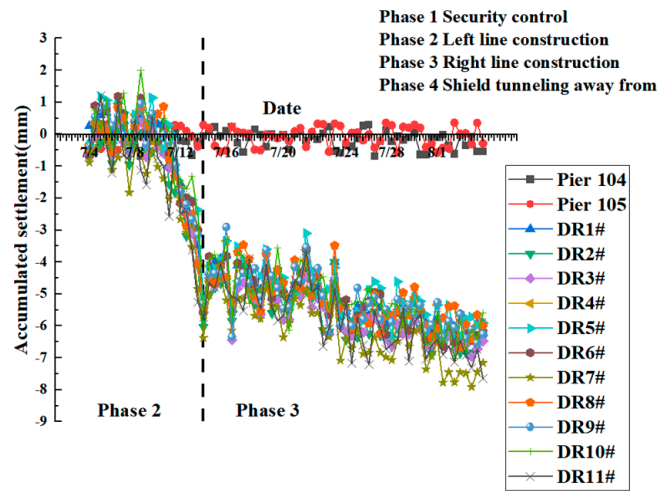


Figure 13. Final surface settlement of the shield tunnel crossing along the left line.

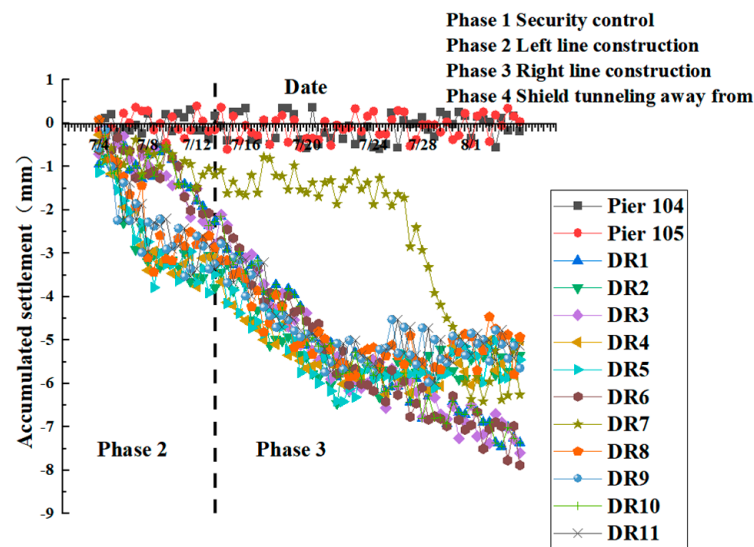


Figure 14. Final surface settlement of the shield tunneling along the right line.

4.2.2. Analysis of Stress Monitoring Results for Pipe Segments

This article conducts stress monitoring on rings 532 and 534, located under segment numbers, respectively. The two ring pipe segments are located directly below the elevated bridge, and reinforcement meters are arranged for the circumferential and longitudinal steel bars on the outer and inner sides, respectively, to measure stress. Its position is close to the inner and outer curved surfaces of the pipe segment, located in the middle of the steel cage on the inner and outer curved surfaces of the pipe segment. The stress situation between the two ring segments is basically the same. Below, we choose to analyze the data from ring 534, where the positive and negative stress values represent the direction, and the positive value represents the stress pointing from the soil towards the pipe segment.

As shown in Figures 15 and 16, the initial stress of the circumferential steel bars inside this ring fluctuates within the range of 4 MPa. Subsequently, the overall trend showed a relatively uniform downward fluctuation, and the later stage remained stable within the

range of -2 MPa. During the final monitoring period, there were small-scale fluctuations in the growth rate. The overall fluctuation range of stress remains within $(-6, 8)$ MPa, and the stress of steel bars basically meets the allowable value. The stress of the outer circumferential steel bar is similar to that of the inner circumferential steel bar and fluctuates at higher stress positions in the initial stage. The highest value is close to 9 MPa, slightly higher than the peak stress on the inner side. Subsequently, there was also a relatively uniform downward trend of fluctuations, with stable fluctuations maintained at -2 MPa in the later stage. Similarly, during the final monitoring period, there was a small range of amplitude fluctuations, and the overall stress remained within the range of $(-4, 9)$. The stress of the steel bars basically met the allowable value.

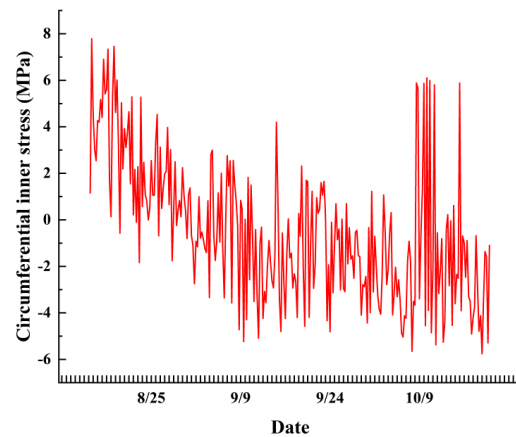


Figure 15. Stress on the inner side of ring 534.

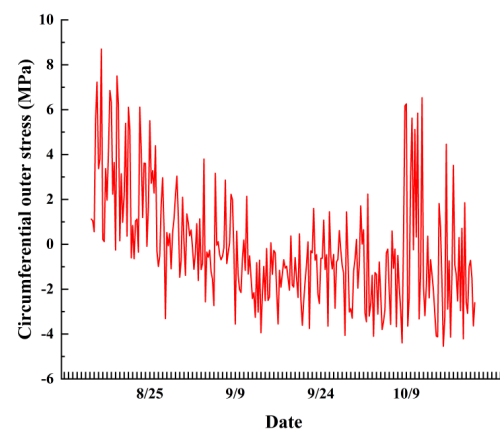


Figure 16. Stress on the outer side of ring 534.

As shown in Figures 17 and 18, there is a significant stress peak in the longitudinal reinforcement on the inner side of this ring at the initial entry position. The highest value reached 16 MPa, but only appeared once. Subsequently, the overall trend showed a relatively stable downward fluctuation, and the stress in the later stage remained stable within the range of 0 MPa, fluctuating and changing. The overall fluctuation range of longitudinal steel bar stress is within the range of $(-5, 15)$ MPa. The stress of steel bars basically meets the allowable value. The stress variation trend of the outer longitudinal steel bars is relatively close to that of the inner side. However, the time of peak stress occurrence has shifted backwards, and the overall fluctuation amplitude is greater, with the stress significantly higher than the inner side. The overall fluctuation range is within the range of $(-3, 17)$ MPa, and the stress of the steel bars basically meets the allowable value.

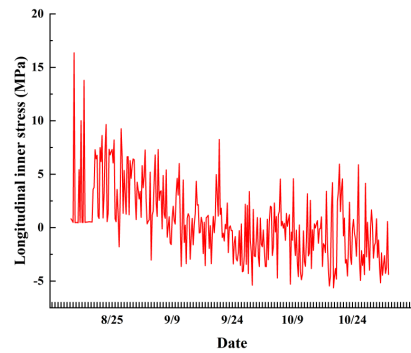


Figure 17. Longitudinal inner stress of ring 534.

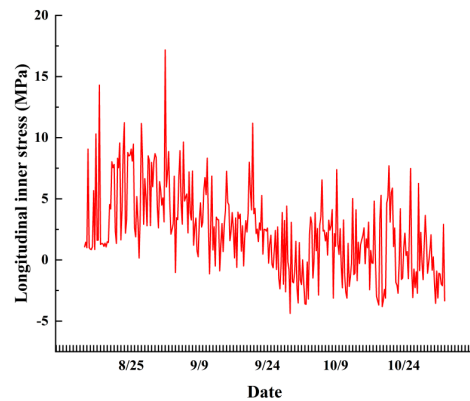


Figure 18. Longitudinal outer stress of ring 534.

4.2.3. Analysis of Soil Pressure Monitoring Results

This article conducts soil pressure stress monitoring on rings 532 and 534, respectively, located in the pipe segment number. The two ring segments are located directly below the elevated bridge, and an earth pressure box is buried behind the outer segment. Its position is close to the outer curved surface of the pipe segment, and the stress situation of the two ring pipe segments is basically the same. Next, we will analyze the data from ring 534, where positive and negative values represent the direction, and positive values represent the pressure exerted by the soil on the pipe segment.

As shown in Figure 19, the soil pressure on this ring pipe segment has been maintained in a stable range during the early stage and undergoes slight fluctuations. It can be basically determined that the soil has not been disturbed during this period. Hence, the soil pressure exhibits a stable state. Subsequently, there was a certain fluctuation in the later stage of monitoring, with a peak value close to -0.6 MPa. Finally, it returns to the initial stress state, and the soil pressure on the entire process is within the allowable range.

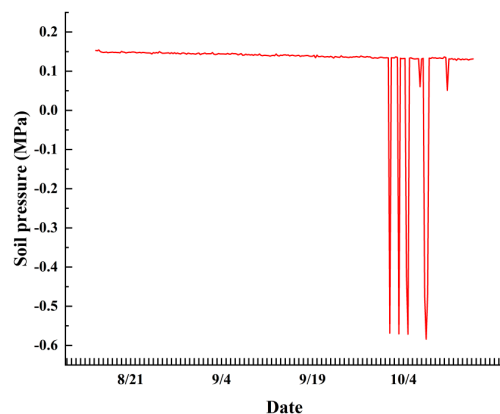


Figure 19. Soil pressure on the ring 534 pipe segment.

5. Conclusions

Using By combining on-site monitoring and numerical simulation methods. Simulate disturbance under normal excavation conditions before excavation. Based on simulation results, safety control measures will be taken for on-site excavation by monitoring surface settlement, pipe stress, and soil pressure on site. The evaluation of the impact of small-radius stacked tunnels crossing elevated bridges has led to the following conclusions:

1. Through disturbance simulation under normal excavation conditions, it was found that as the shield tunneling construction continued to advance, the cumulative settlement value of the bridge piers eventually exceeded the warning value by 1 mm. Security control measures must be taken.
2. The settlement variation law of bridges is closely related to the spatial position of bridges and tunnels. In the area close to the tunnel, there is a significant change in surface settlement during the shield tunneling construction phase, and the force fluctuations on the pipe segments are significant. At this stage, the proportion of changes in surface settlement on the mainland to total settlement is relatively high. In areas far from the tunnel, significant changes in settlement occur during the tunneling phase of shield tunneling construction. The settlement variation during this stage accounts for a relatively high proportion of the total settlement.
3. The monitoring results of shield tunneling through elevated bridges after implementing safety control measures show that the deformation of the bridge and surface settlement are significantly reduced. The stress situation of the pipe segments is within the allowable range and meets the safety control standards. Verified the effectiveness of security control measures.
4. During construction, the grouting method can adopt a sequential hole pattern, and it is best to use the grouting construction method of interval jumping holes, gradual constraint, and first from bottom to top. During grouting construction, 3–5 leveling observation points should be set up on the surface for monitoring, and cracks and uplift are not allowed to occur on the ground. Once cracks and uplift occur on the ground, the grouting pressure and amount must be adjusted in a timely manner.

Author Contributions: Conceptualization, T.Y. and X.P.; methodology, T.Y.; software, X.P.; validation, X.H. and B.L.; formal analysis, X.H., B.L. and T.W.; investigation, T.Y.; resources, X.P.; data curation, T.Y.; writing—original draft preparation, X.P.; writing—review and editing, T.Y.; project administration, K.L., J.Z. and Y.L. All authors have read and agreed to the published version of the manuscript.

Funding: This research was supported by the National Natural Science Foundation of China (Grant Nos. 52074258 and U22A20234), Hubei Provincial Natural Science Foundation Outstanding Youth Project (Grant No. 2022CFA084), Hubei Provincial Key Research and Development Program (Grant No. 2021BCA133), Wuhan City Knowledge Innovation Special Project (Grant No. 2022010801010162), and Youth Innovation Promotion Association member program of Chinese Academy of Sciences.

Institutional Review Board Statement: Not applicable.

Informed Consent Statement: Informed consent forms have been obtained from all participants in the study.

Data Availability Statement: The data presented in this study are available on request from the corresponding author due to detailed data involves some privacy.

Conflicts of Interest: The author Yang Taihua is employed by the School of Urban Construction at Wuhan University of Science and Technology. The remaining authors declare that the study was conducted in the absence of any commercial or financial relationships that could be interpreted as potential conflicts of interest.

References

1. Zhang, Z.Q.; He, C. Research on key technique of shield tunnel construction beneath adjacent existing highway tunnel. *Rock Soil Mech.* **2005**, *26*, 20–25.
2. Fan, H.B. A study of the influence of shield tunnelling on surrounding environment based on the overlay model. *Chin. J. Rock Mech. Eng.* **2005**, 1092. [[CrossRef](#)]
3. Wang, M.Q.; Chen, S.H. 3-Dimensional non-linear finite element simulation of tunnel structure for moving-forward shield. *Chin. J. Rock Mech. Eng.* **2002**, *21*, 228–232. [[CrossRef](#)]
4. Zhao, X.F.; Wang, C.M.; Sun, J.L.; Kong, X.L. Analysis of mechanical action of shield driving for approaching excavation. *Rock Soil Mech.* **2007**, *21*, 409–414.
5. He, C.; Su, Z.X.; Zeng, D.Y. Influence of metro shield tunneling on existing tunnel directly above. *China Civ. Eng. J.* **2008**, 91–98.
6. Peck, R.B. Deep Excavation and Tunnelling in Soft Ground. State of the Art Report. In Proceedings of the 7th International Conference on Soil Mechanics and Foundation Engineering (Mexico), Mexico City, Mexico, 25–29 August 1969; pp. 225–290.
7. Chen, C.L.; Zhao, C.L.; Wei, G.; Ding, Z. Prediction of soil settlement induced by double-line shield tunnel based on Peck formula. *Rock Soil Mech.* **2014**, *35*, 2212–2218.
8. Lu, C.; Zhang, X.; Shi, B.; Jiang, J.; Lin, Z. Deformation in settlement and grouting remediation of thickened larger-diameter metro shield tunnel in soft soil: A case study. *Case Stud. Constr. Mater.* **2024**, *20*, e02736. [[CrossRef](#)]
9. Wang, Q.; Xie, X.Y.; Huang, Z.H.; Qi, Y. Study of settlement troughs over quadruple-tube parallel shield tunnels crossing railway tracks. *Chin. J. Rock Mech. Eng.* **2017**, *S2*, 4235–4243.
10. Osman, A.S.; Mair, R.J.; Bolton, M.D. On the kinematics of 2D tunnel collapse in undrained clay. *Geotechnique* **2006**, *56*, 585–595. [[CrossRef](#)]
11. Osman, A.S. Stability of unlined twin tunnels in undrained clay. *Tunn. Undergr. Space Technol.* **2010**, *25*, 290–296. [[CrossRef](#)]
12. Wei, G. Research on theoretical calculation of long-term ground settlement caused by shield tunneling. *Chin. J. Rock Mech. Eng.* **2008**, *27*, 2960.
13. Wei, X.J.; Zhang, J.J.; Zhang, S.M. Grope for shield tunnel construction induced ground maximal settlement. *Rock Soil Mech.* **2008**, *29*, 161–164.
14. Wang, F.; Miu, L.C.; Li, C.L. Numerical analysis of shield tunnel settlement considering construction process. *Chin. J. Rock Mech. Eng.* **2013**, *z1*. [[CrossRef](#)]
15. Teng, L.; Zhang, H. Meso-macro analysis of surface settlement characteristics during shield tunneling in sandy cobble ground. *Rock Soil Mech.* **2012**, *33*, 186–195+205.
16. Takahashi, K.; Fukazawa, N.; Hagiwara, T. Observational control of slurry shield tunnels with super close spacing under the nearby bridge abutments loads. *Tunn. Undergr. Space Technol.* **2004**, *19*, 390.
17. Sirivachiraporn, A.; Phienwej, N. Ground movements in EPB shield tunneling of Bangkok subway project and impacts on adjacent buildings. *Tunn. Undergr. Space Technol. Inc. Trenchless Technol. Res.* **2012**, *30*, 10–24. [[CrossRef](#)]
18. Basile, F. Effects of tunnelling on pile foundations. *Soils Found.* **2014**, *54*, 280–295. [[CrossRef](#)]
19. Jongpradist, P.; Kaewsri, T.; Sawatparnich, A.; Suwansawat, S.; Youwai, S.; Kongkitkul, W.; Sunitsakul, J. Development of tunneling influence zones for adjacent pile foundations by numerical analyses. *Tunn. Undergr. Space Technol. Inc. Trenchless Technol. Res.* **2013**, *34*, 96–109. [[CrossRef](#)]
20. Loganathan, N.; Poulos, H.G.; Stewart, D.P. Centrifuge model testing of tunneling-induced ground and pile deformations. *Géotechnique* **2000**, *50*, 283–294. [[CrossRef](#)]
21. Leung, C.F.; Lim, J.K.; Shen, R.F.; Chow, Y.K. Behavior of Pile Groups Subject to Excavation-Induced Soil Movement. *J. Geotech. Geoenviron. Eng.* **2003**, *129*, 58–65. [[CrossRef](#)]
22. Ong, D.E.L.; Leung, C.F.; Chow, Y.K. Behavior of Pile Groups Subject to Excavation-Induced Soil Movement in Very Soft Clay. *J. Geotech. Geoenviron. Eng.* **2009**, *135*, 1462–1474. [[CrossRef](#)]

Disclaimer/Publisher’s Note: The statements, opinions and data contained in all publications are solely those of the individual author(s) and contributor(s) and not of MDPI and/or the editor(s). MDPI and/or the editor(s) disclaim responsibility for any injury to people or property resulting from any ideas, methods, instructions or products referred to in the content.